

TNO-report

93-CMC-R0786

REDUCED STIFFNESS METHOD FOR ONSET OF DELAMINATION

TNO Building and
Construction Research

Lange Kleiweg 5, Rijswijk
P.O. Box 49
2600 AA Delft
The Netherlands

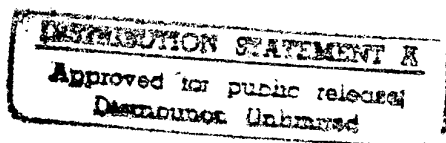
Phone +31 15 284 20 00
Fax +31 15 284 39 90
Telex 38270

Date 30 August 1996

Author(s) ir. J. van den Eikhoff

Sponsor: Ministry of Defence
Directie Materiaal KM
Afdeling Scheepsbouw
Postbus 20702
2500 ES 's-Gravenhage

Monitoring agency: TNO Defence Research



Security Classification
decided by : ir. T.N. Bosman
dated : 16 February 1996

Title : ONGERUBRICEERD
Managementuittreksel : ONGERUBRICEERD
Abstract : ONGERUBRICEERD
Report text : ONGERUBRICEERD
Appendices : ONGERUBRICEERD

All rights reserved.
No part of this publication may be
reproduced and/or published by print,
photoprint, microfilm or any other
means without the previous written
consent of TNO.

In case this report was drafted on
instructions, the rights and obligations
of contracting parties are subject to
either the Standard Conditions for
Research Instructions given to TNO
or the relevant agreement concluded
between the contracting parties.
Submitting the report for inspection to
parties who have a direct interest is
permitted.

The classification designation 'ONGERUBRICEERD' is
equivalent to 'UNCLASSIFIED'.

Project name : Ontwerpmethoden composiet
scheepsconstructies
Projectnumber : 42775554 - A92/KM/178
Approved : ir. G.J. Meijer
Visa : ir. G.T.M. Janssen

© TNO

Pages : 22 (excl. RDP & distribution list,
incl. Appendices)

DTIC QUALITY INSPECTED 3

TNO Building and Construction Research provides a
comprehensive research and development service
specifically geared to the needs of the construction and
engineering industry.



Netherlands Organization for
Applied Scientific Research (TNO)

The Standard Conditions for Research Instructions
given to TNO, as filed at the Registry of the District Court
and the Chamber of Commerce in The Hague
shall apply to all instructions given to TNO.

19970212 047

Managementuittreksel

Titel: **Reduced stiffness method for onset of delamination**
Auteurs: J. v.d. Eikhoff;
Datum: 30 Augustus 1996
Opdrachtnummer: 42775554 - A92/KM/178
IWP-nr: 792
Rapportnummer: 93-CMC-R0786

Aanleiding van het onderzoek

De wens de specifieke voordelen van glasvezel versterkte kunststoffen op uitgebreidere schaal te benutten.

Doel van het onderzoek

Het ontwikkelen van kosteneffectieve oplossingen voor ontwerp en fabricage van composiet constructies in de scheepsbouw, waarmee deze constructies op veel grotere schaal toegepast kunnen worden en bovendien een langere levensduur hebben.

Korte omschrijving

Een methode uit de literatuur "de gereduceerde stijfheidsmethode" is bestudeerd en gebruikt om van verschillende grafiet-epoxy laminaten het begin van delaminatie te bepalen.

Conclusies en aanbevelingen

De gereduceerde stijfheidsmethode is gebruikt om het begin van delaminatie van een aantal laminaten van AS4/3501.6, T300/934 en T300/5208 grafiet- epoxy platen te bepalen. De resultaten zijn veelbelovend. Het voordeel is dat het niet nodig is om gedetailleerde spanningen in de derde richting en lokale spanningen aan het oppervlak van de plaat te berekenen. Ten einde de methode bruikbaar te maken voor de eindige-elementen methode is het nodig situaties met variërende spanningen te onderzoeken. Ook is het mogelijk dat het begin van delaminatie verschillend zal zijn voor de twee loodrechte richtingen van het laminaat. In gevallen waar beide (loodrechte) spanningen dicht bij de kritieke delaminatie spanning liggen, zullen ze waarschijnlijk interactie vertonen. Ook de interactie tussen matrix scheuren en delaminatie moet verder onderzocht worden.

CONTENTS

Managementuittreksel	2
CONTENTS	3
1 INTRODUCTION	4
2 THEORY	4
3 EXAMPLES	7
Comparison with theory for $[\pm 25/90]_s$ layup of AS4/3501.6 graphite epoxy	7
Delamination growth in $[\pm 30 \pm 30/90_{1/2}]_s$ layups of T300/5208 graphite epoxy	9
Thickness influence in $[\pm 45_0/0_0/90_n]_s$ layups of T300/5208 graphite epoxy	11
Damage interaction in $[\pm 25/90_n]_s$ layups of T300/934 graphite epoxy	13
Damage interaction in $[0_2/90_n]_s$ layups of T300/934 graphite epoxy	16
4 DISCUSSION AND RECOMMENDATIONS	17
5 LITERATURE	18
Appendix 1 Longitudinal laminate stiffness for "Natural boundary conditions"	19
Appendix 2 Longitudinal laminate stiffness for "Alternating delamination boundary conditions"	19
Appendix 3 Longitudinal laminate stiffness for "moment free boundary conditions"	21
Appendix 4 Longitudinal laminate stiffness for "curvature free boundary conditions"	22

1 INTRODUCTION

In this report some aspects of delamination (separation of laminate plies) are considered. If a laminate is loaded in its plane it may happen that two plies separate. Because the various plies in the laminate contract differently perpendicular to the loading, stresses in the other directions arise. Near the boundary shear stresses are necessary to build up these inplane stresses. Moreover in the third direction stresses arise to prevent the laminate to bend due to the inplane stresses. Due to the combined influence of shear forces and the stresses in the third direction delamination may arise. This may lead to a significant loss of stiffness. The reduced stiffness method has been used to determine the onset of delamination in a laminate. This theory has the advantage that detailed calculations of the stresses in the other directions are not necessary. It will be outlined in Chapter 2. With the theory we calculate the onset of delamination in a number of different layups of some graphite epoxy layups, for which data were available. The results are presented in Chapter 3. Finally we discuss the results and give some recommendations in Chapter 4.

2 THEORY

If the plies of a laminate separate (called delamination), its longitudinal laminate stiffness (in the loading direction) reduces. The energy which is released by this stiffness reduction is used to create the new (delamination) surface. O'Brien [1] used this reduced stiffness method to determine the onset of delamination. The theory will be explained using the next figure.

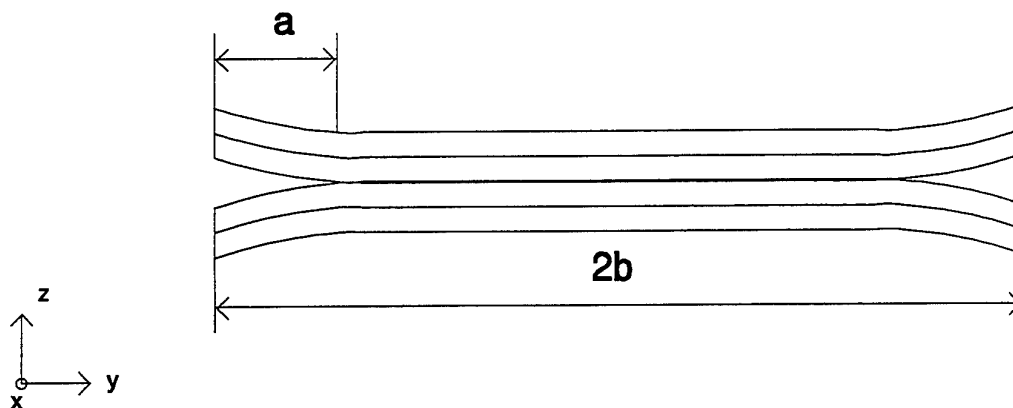


Figure 1 Partially delaminated specimen

A specimen, consisting of a number of plies with different fibre directions, has been delaminated at both sides over a certain distance. The specimen is loaded in the longitudinal (x-)direction (perpendicular to the plane of this figure). The effective stiffness in this direction of this specimen can be approximated as:

$$E_p = (E_d - E_i) \frac{a}{b} + E_i = (E_d - E_i) D_d + E_i \quad (1)$$

where:

- E_p : Stiffness of partially delaminated specimen [Pa];
- E_i : Stiffness undamaged specimen [Pa];
- E_d : Stiffness totally delaminated specimen [Pa];
- $2b$: Width of the specimen [m];
- a : Delamination length at each side [m].
- D_d : Damage parameter for delamination [-].

This approximation is valid as long as the undelaminated part is large compared to the thickness. The ratio of a and b is a delamination damage parameter D_d , which is 1 for total delamination. It will be used for damage growth later on. The amount of stored energy π in the specimen is (the strains in the y and z-directions are unimportant because there is no external load in that directions):

$$\pi = \int_V \frac{1}{2} \epsilon_i C_{ij} \epsilon_j dV = \int_V \frac{1}{2} \epsilon_x^2 E_p dV \quad (2)$$

$$V = 2 b l t$$

where:

- C : Stiffness tensor [Pa];
- ϵ_x : Strain in the longitudinal direction [-];
- V : Volume [m³];
- l : Length of the specimen [m];
- t : Thickness of the laminate [m].

The energy release rate G_d is:

$$G_d = - \frac{\partial \pi}{\partial A} = - \frac{\partial (\epsilon_x^2 E_p b l t)}{\partial (2 a l)} = - \frac{\epsilon_x^2 b t}{2} \frac{\partial E_p}{\partial a} = - \frac{\epsilon_x^2 (E_d - E_i) t}{2} \quad (3)$$

$$A = 2 a l$$

where:

- A : Delaminated surface [m²];

With this equation the strain ϵ_c where delamination initiates can be determined from the critical energy release rate G_{dc} (or G_{dc} from an experimental ϵ_c):

$$\epsilon_c = \sqrt{\frac{2 G_{dc}}{t(E_i - E_d)}} \quad (4)$$

where:

- ϵ_c : Delamination initiation strain [-];
- G_{dc} : Energy release rate at delamination initiation [N/m].

Damage growth is treated in the same way as for matrix cracks as reported by Paas and van den Eikhoff [2]. A thermodynamic force for delamination X_d is defined by:

$$X_d = -\frac{\partial \psi}{\partial D_d} = -\frac{\partial \frac{\pi}{V}}{\partial D_d} = -\frac{\partial (\frac{1}{2} \epsilon_x^2 E_p)}{\partial D_d} = \frac{1}{2} (E_i - E_d) \epsilon_x^2 = \frac{G_d}{t} \quad (5)$$

where ψ is the specific stored energy.

If we choose a dissipation potential ϕ linear in the thermodynamic force:

$$\begin{aligned} \phi &= A_d X_d - D_d X_d^0 \\ X_d^0 &= \frac{G_{dc}}{t} \end{aligned} \quad (6)$$

with:

A_d : Material/construction parameter for delamination expansion [-];
 X_d^0 : Threshold value for delamination growth [N/m²];

This potential can be used to determine the delamination damage as a function of strain in an analog way as in [2]:

$$D_d = \frac{a}{b} = A_d \left(\frac{X_d}{X_d^0} - 1 \right) = A_d \left(\frac{G_d}{G_{dc}} - 1 \right) = A_d \left(\frac{\epsilon_x^2}{\epsilon_c^2} - 1 \right) \quad (7)$$

The "strain at total delamination ϵ_d " can be determined by substituting $D_d = 1$ ($a=b$) in (7):

$$\epsilon_d = \epsilon_c \sqrt{1 + \frac{1}{A_d}} \quad (8)$$

The values for E_i en E_d have been calculated for a number of layups with PLAMOR. During this project it became clear that there is a lot of confusion which stiffness term has to be used. We will now shortly indicate this problem.

For a general laminate we have the following relation between laminate forces and moments on the one hand and the midplane strain and curvature at the other hand:

$$\begin{bmatrix} N \\ M \end{bmatrix} = \begin{bmatrix} A & B \\ B^T & D \end{bmatrix} \begin{bmatrix} \epsilon \\ \kappa \end{bmatrix} \quad (9)$$

where:

N : Forces on the laminate [N_x, N_y, N_{xy}]^T;
 M : Moments on the laminate; [M_x, M_y, M_{xy}]^T;
 ϵ : Strain in the midplane; [$\epsilon_x, \epsilon_y, \epsilon_{xy}$]^T;
 κ : Curvature of the midplane [$\kappa_x, \kappa_y, \kappa_{xy}$]^T.

For the reduced stiffness we are only interested in the reaction force in the load direction on a strain in that direction. However this reaction force will depend on the other boundary conditions of the laminate. If we constrain ourselves to symmetrical laminates which are partly delaminated from the edges and loaded in one direction, than we have the following boundary conditions:

- A) Natural boundary conditions in the delaminated part
The delaminated parts can freely extend in the y-direction (in the plane of the laminate perpendicular to the load) ($N_y=0$) and they can bend freely about the x-axis ($M_y=0$). It can not shear around the z-axis ($\epsilon_{xy}=0$) and probably there will be no twist ($\kappa_{xy}=0$), furthermore the faces will remain approximately straight ($\kappa_x=0$). The details of the determination of the longitudinal (x) laminate stiffness are given in Appendix 1.
- B) Alternating delamination boundary conditions
From experiments it follows that sometimes the delamination switches up and down between two symmetric interfaces in the length of the specimen. O'Brien [1] believes that "Delaminations grow in this matter to reduce the effect of bending-extension coupling". This means that internally there may be a (opposite) curvature in two adjacent parts of the laminate, giving a nett effect of approximately no curvature. The longitudinal laminate stiffness is given in Appendix 2.
- C) Free boundary conditions
Schellekens [3] uses a formula for the effective stiffness which is equivalent with the assumption that all the moments and N_y and N_{xy} are zero. From (9) the curvatures can than be eliminated giving the equations of Appendix 3.
- D) Curvature free boundary conditions
O'Brien [1] found that using the free boundary conditions gives results that are not stiff enough and he proposes to discard the bending extension coupling, which is the same as demanding that all the curvatures are zero, see Appendix 4.

It is the opinion of the author that the boundary conditions A) and B) are the right ones to use, whichever gives the lowest delamination initiation strain.

3 EXAMPLES

In this chapter we apply the theory of the previous chapter for a number of different graphite epoxy laminates to calculate the delamination initiation strain and for which experimental or numerical data were available. The program PLAMOR developed at the TU Delft has been used to determine the stiffnesses of the laminates. In Section 3.1 we focus on the comparison with theoretical calculations. Delamination growth is the major topic in Section 3.2. Thickness effects is the topic in Section 3.3. Sections 3.4 and 3.5 show that interaction with matrix cracking or fibre break is important for certain laminates.

3.1 Comparison with theory for $[\pm 25/90]_s$ layup of AS4/3501.6 graphite epoxy

In this section we compare the reduced stiffness results with results of calculations by Schellekens en de Borst [3] with a $[\pm 25/90]_s$ layup of AS4/3501.6 graphite epoxy. They gave the following material data:

E_1 : 140 GPa;
 E_2 : 11 GPa;

G_{12} : 5.5 GPa;
 ν_{12} : 0.29;
ply thickness : 0.132 mm.

For a number of layups the effective E_x has been determined with PLAMOR and the formulas of Appendix 1 and 3. The results are given in the next table for Free boundary conditions (App. 3) used in [3] and "Natural boundary conditions" (App 1), which should have been used according to the author.

Layup Boundary conditions	E_x [GPa]	
	Free	Natural
[25]	29.6	71.0
[25/-25]	42.4	71.4
[25/-25/90]	36.1	55.5
[25/-25/90/90]	25.0	47.0
[25/-25/90/90/-25]	34.4	59.7
[25/-25/90] _s	66.0	66.0

It is obvious that the boundary conditions have an enormous influence on the longitudinal laminate stiffness, the free conditions being much less stiff. By taking combinations of two layups (e.g. [25/-25/90/90] and [25/-25]) and the corresponding value for E_x , E_d for a complete delaminated layup can be determined with delaminations at different interfaces:

$$E_d = \frac{n E_x^n + m E_x^m}{n+m} \quad (10)$$

where:

E_x^n : E_x of the part with n plies;
 E_x^m : E_x of the part with m plies;

Next we can calculate with (4) the critical strain where delamination would start in the different interfaces. The results are given in the next table. We used $G_{dc}=350$ N/m [3] (supposed to be independent of the angle between the fibres in adjacent plies).

Boundary condition	Free ^{*)}		Natural ^{*)}	
Layup	E_d [GPa]	ϵ_c [-]	E_d [GPa]	ϵ_c [-]
[25/-25/90/90/-25]+[25]	33.6	.0052	61.6	.00141
[25/-25/90/90]+[-25/25]	30.8	.0050	55.1	.00900
[25/-25/90]+[90/-25/25]	36.1	.0054	55.5	.00917
[25/-25/90/90]+[-25/25]	Alternating delam ^{*)} :		54.9	.00891

^{*)} See Chapter 2 and the Appendices

From this table follows that there is little preference for delamination at the different interfaces (ϵ_c is almost equal), but delamination between a 90-layer and a -25-layer will probably start first, preferably alternating between the two symmetric interfaces. The influence of the boundary conditions is tremendous, approximately a factor 2 in the delamination initiation strain.

In [3] it was found that for a (non-linear) fracture mechanics approach with plane strain elements and 3-D line interface elements a critical strain was found of approximately .009 for a delamination in the midplane. For the natural boundary conditions and the reduced stiffness method we find almost the same initiation strain. In order to get the same answer with (4) and the **free boundary conditions** one should use a G_{dc} of 970 N/m. Schellekens, who used these conditions for the reduced stiffness, concluded that "this cast some doubt on the merit of the reduced stiffness approach in predicting the onset of delamination". We now can conclude that the results of this method and the Finite Element Method match perfectly, provided the same boundary conditions are used in both. We must also conclude that it is dangerous to rely on symmetry conditions because unlike the assumptions in the Finite Element calculations the delamination will probably not start in the midplane of the laminate and may not even be on the same side of the midplane over the whole length of the specimen.

3.2 Delamination growth in $[\pm 30 \pm 30 / 90]_{1\frac{1}{2}}$ layups of T300/5208 graphite epoxy

Now we deal with an example of $[\pm 30 \pm 30 / 90]_{1\frac{1}{2}}$ layups of T300/5208 graphite epoxy as presented by O'Brien [1]. The material data were given as:

E_1 : 138 GPa;
 E_2 : 15 GPa;
 G_{12} : 5.9 GPa;
 ν_{12} : 0.21;
 ply thickness : 0.137 mm.

From this data we calculated, for the natural boundary conditions:

Layup	E_x [GPa]
$[\pm 30]_2$	53.8
$[90]_3$	15.0
$[\pm 30 / \pm 30 / 90]_3$	41.6
$[\pm 30 / \pm 30 / 90]_{1\frac{1}{2}}$	47.0
$[\pm 30 / \pm 30 / 90]_3 / \pm 30 / \pm 30$	58.2

and:

Layup	E_1 [GPa]	E_d [GPa]	ϵ_c [-]	ϵ_c [-] experim.
$[\pm 30/\pm 30/90_3] + [\pm 30]_2$	58.2	46	.00376	.0035
$[\pm 30]_2 + [90_3] + [\pm 30]_2$	58.2	43.2	.00479 *	.0035
$[\pm 30/\pm 30/90_{1\frac{1}{2}}] + [90_{1\frac{1}{2}}/\pm 30/\pm 30]$	58.2	47.0	.00392	.0035
$[\pm 30/\pm 30/90_3] + [\pm 30]_2$ (alternating)	58.2	45.9	.00374	.0035

* *Here two delamination surfaces arise.*

A value of $G_{dc}=130$ N/m has been determined in [1] to fit the experimental delamination initiation and has been used with (4) to determine the delamination initiation strain. This value is much smaller than the value used in the previous examples for AS4/3501.6.

A value for G_{dc} , independent of the experimental data, can be determined as follows:

The critical energy release rate G_{lc} for transverse matrix cracking was found to be [2]:

- 64 N/m for AS4-3501.6
- 31 N/m for T300/934 .

Assuming that the same ratio will hold for the critical release rate in delamination, $G_{dc} = 170$ N/m ($31/64 \cdot 350$) can be used, giving an (alternating) delamination initiation strain of .0043 in reasonable accordance with the experimental data.

[1] also gives the development of G_d versus the relative delaminated surface (i.e. the delamination damage) as shown in the next Figure.

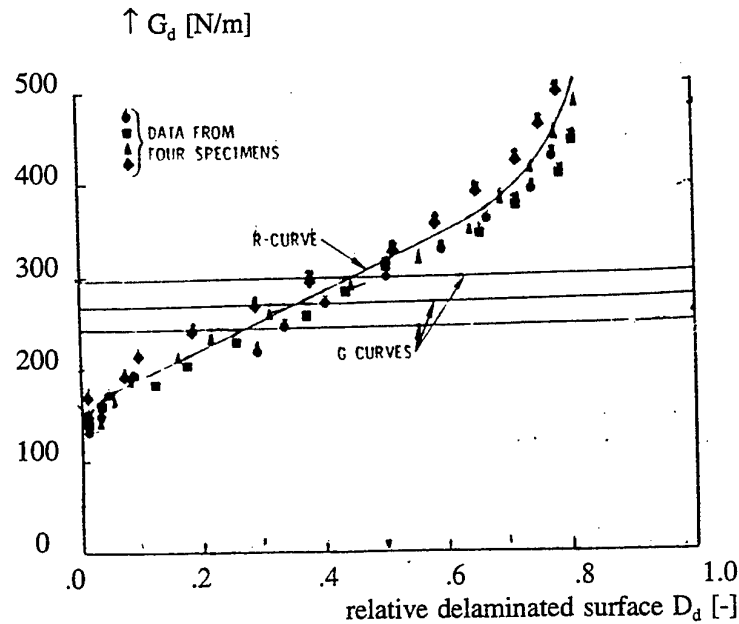


Figure 2 Delamination resistance curve for $[\pm 30/\pm 30/90_3/\pm 30/\pm 30]$ T300-5208 graphite-epoxy laminates.

Using Equation (7) we see that a large part of the resistance curve (up to a damage of 0.7) can be fitted using $A_d = 0.5$ and $G_{dc} = 160$ N/m (which is very close to the value of 170 N/m which was found as a prediction). G_d increases during delamination growth. From this figure it can also be seen that delamination growth starts in the experiments for G_d between 130 and 200 N/m. For damages above 0.7 the resistance curves bend upwards.

3.3 Thickness influence in $[\pm 45_\pi/0_\pi/90_\pi]_s$ layups of T300/5208 graphite epoxy

O'Brien [1] also gives results for $[\pm 45_\pi/0_\pi/90_\pi]_s$ layups of T300/5208 graphite epoxy. The material data were the same as in the previous example, however the ply thickness was 0.15 mm.

For the various layups we find:

Layup	E_x [GPa]
[45]	20.6
[±45]	20.9
[±45/0]	60.4
[±45/0/90]	49.3
[±45/0/90 ₂]	43.0
[±45/0/90 ₂ /0]	59.4
[±45/0/90 ₂ /0/-45]	58.7
[±45/0/90 ₂ /0/±45]	55.7

We determined the critical strain in the various interfaces for the same $G_{dc}=130$ N/m:

Layup	E_i [GPa]	E_d [GPa]	ϵ_c [-]
[45]+[±45/0/90 ₂ /0/-45]	55.7	53.9	.0108
[±45]+[±45/0/90 ₂ /0]	55.7	49.8	.0060
[±45/0]+[±45/0/90 ₂]	55.7	49.5	.0059
[±45/0/90]+[±45/0/90]	55.7	49.3	.0058

From this table it follows that delamination most likely will start in the surface of symmetry. For this layup an alternating delamination was not predicted. For three different thicknesses we compare the results with the experimental delamination initiation strains given in [1].

n	ϵ_c [-] theory	ϵ_c [-] experiment
1	.0058	.0058
2	.0041	.0047
3	.0033	.0036

We can conclude that the correspondence between experimental value and predicted value is good although the G_{dc} from another layup has been used.

3.4 Damage interaction in $[\pm 25/90]_n$ layups of T300/934 graphite epoxy

Crossman and Wang [4] give results for $[\pm 25/90]_n$ layups of T300/934 graphite epoxy for different thicknesses of the 90-layer. We used their material data:

E_1 : 145 GPa;
 E_2 : 11.7 GPa;
 G_{12} : 6.5 GPa;
 ν_{12} : 0.3.

No thickness was reported, we used $t=0.132$ mm.

For a number of layups the effective E_x is calculated with PLAMOR for the natural boundary conditions and for the alternating boundary conditions. From these values the delamination initiation strain can be calculated and, with the initial stiffness, the delamination initiation stress. The results for an alternating delamination are presented in the next table, because the initial stresses are the lowest. The results are compared with the experimental stresses in the next table using the same $G_{dc}=130$ N/m as in the previous example (but a different epoxy). The layup with the lowest initiation stress has been presented. It appears that delamination is predicted at the 90/25 interface for all n . For $n<3$ delamination in the surface of symmetry is almost as likely. This is in agreement with the experiments where both arise (sometimes even alternating) for $n<3$. For $n>3$ two alternating delaminations arise are seen in the experiments. For those thick 90-layers delamination starts along the transverse cracks indicating that these two damage modes interact.

From the calculations follows, that there is little difference between delamination at the symmetry plane and at the -25/90 plane.

Layup	E_1 [GPa]	E_d [GPa]	σ_c [MPa]	σ_c [MPa] experim.
$[\pm 25/90] + [\pm 25]$	77.6	65.9	449	425-457
$[\pm 25/90_2] + [\pm 25]$	69.0	58.3	383	409-413
$[\pm 25/90_4] + [\pm 25]$	55.8	48.1	316	311-332
$[\pm 25/90_6] + [\pm 25]$	47.3	41.3	271	258-287
$[\pm 25/90_8] + [\pm 25]$	41.5	36.6	239	200-216
$[\pm 25/90_{12}] + [\pm 25]$	34.2	30.5	197	125-135
$[\pm 25/90_{16}] + [\pm 25]$	29.8	26.8	172	92.3-97.8
$[\pm 25_2/90_4] + [\pm 25_2]$	69.0	58.3	272	296-308

The calculated initial stiffness is compared with the experimental stiffness in the next Figure 3. The correspondence is very good.

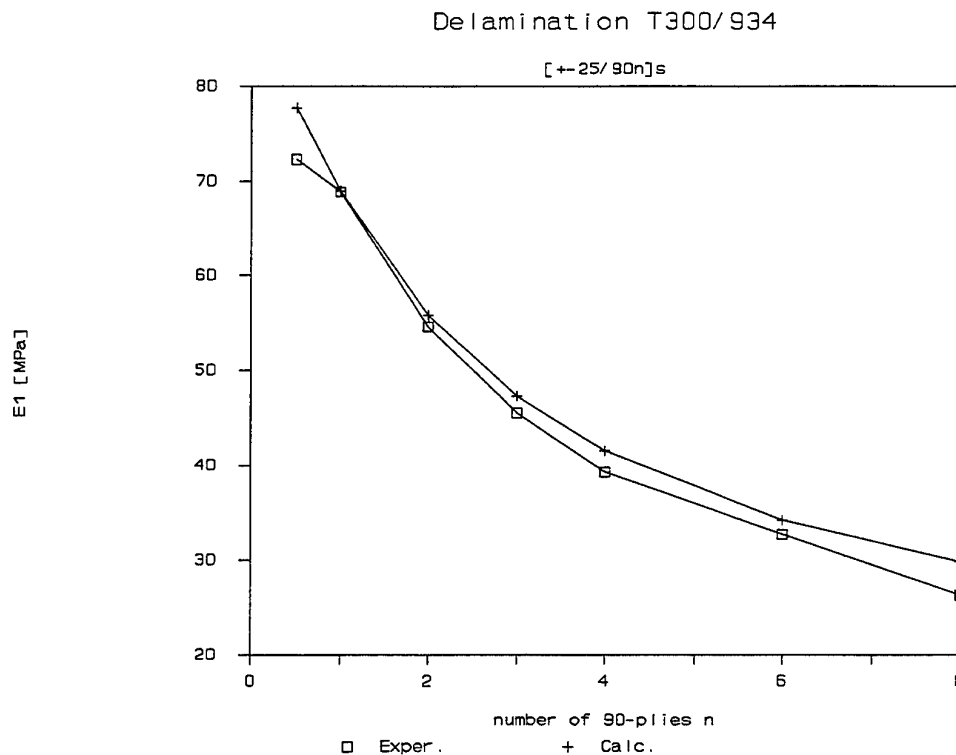


Figure 3 Tangent modulus for [$\pm 25/90_n$]_s T300/934.

The dependence of the delamination initiation **stress** with the number of 90-ply layers is shown in Figure 4 and is compared with the experimental range (lower-upper). The general trend is the same for experiment and calculation, but the mean of the calculated stresses is 16% higher than the mean of the experimental values. Especially for thick laminates the experimental values are lower, probably because of the interaction with the transverse matrix cracks.

Delamination initiation **strain** versus the number of the 90-ply layers is shown in Figure 5 together with the experimental range. The predicted values are very good up to $n=4$. It can be seen that the experimental initiation strain drops for thick layers, whereas the calculated value remains almost constant. For small n (up to 4) the (experimental) initiation strain is 7% below the ultimate strain of a [± 25]_s laminate; for $n=5$ and 6 it is 7% below the ultimate strain of a [90]_s laminate.

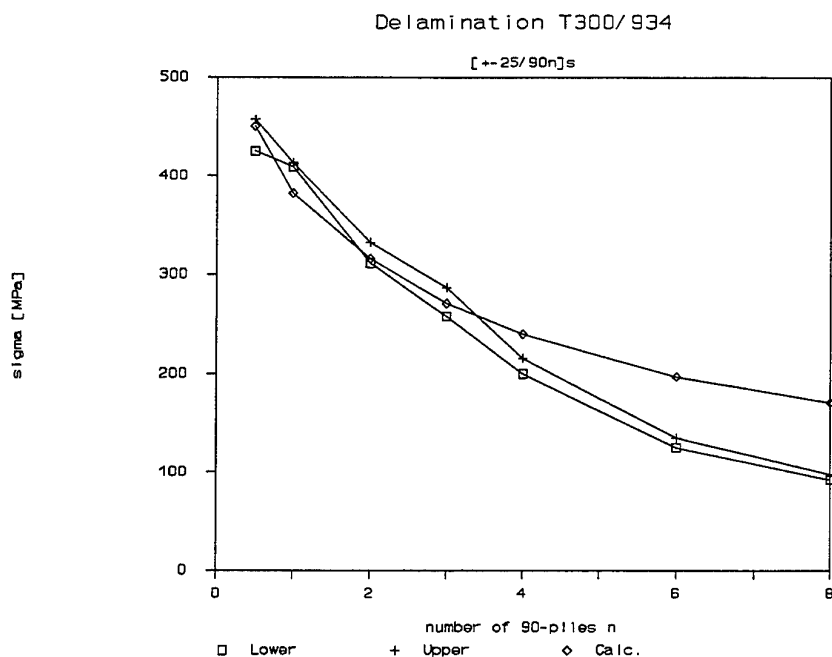


Figure 4 Delamination stress of [$\pm 25/90_n$]_s T300/934.
Lower-Upper: Experimental range.

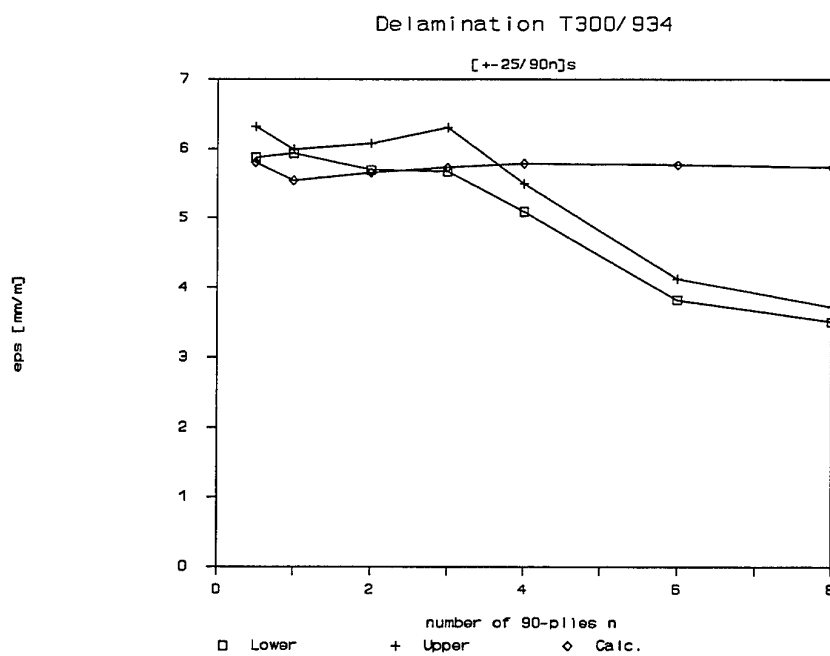


Figure 5 Delamination strain of [$\pm 25/90_n$]_s T300/934.
Lower-Upper: Experimental range.

This drop in initiation strain is probably due to the interaction with the transverse cracks. Because of these cracks the stiffness of the laminate drops considerably, especially for thick 90-layers, giving larger strains than the ones following from the original stiffness. This can also explain why the results for the delamination initiation stress agree better, because the initial stiffness has been used to calculate the initial strains from the experiments. Also the strain in the outer layers is concentrated somewhat over the transverse crack giving a faster initiation.

With the method outlined in [2] we also calculated the onset of transverse matrix cracking. The results are presented in the next table.

Layup	σ_c [MPa] transv. crack	σ_c [MPa] Experimental
[25/-25/90 ₂] _s	250	207-243
[25/-25/90 ₃] _s	171	147-167
[25/-25/90 ₄] _s	131	127
[25/-25/90 ₆] _s	88	98-120
[25/-25/90 ₈] _s	66	85.4-97.8
[25 ₂ /-25 ₂ /90 ₂] _s	320	296-308

The correspondence is good, although the differences in critical stresses are somewhat smaller in the experimental data than in the calculated values. For the thin specimens the onset of transverse matrix cracking is for slightly lower strains, so when delaminations starts there are only a few cracks. For thick laminates however transverse matrix cracking starts at much lower strains. This means that there are much more cracks, which will influence the stiffness and the delamination initiation.

3.5 Damage interaction in [0₂/90_n]_s layups of T300/934 graphite epoxy

Wang, Kishore and Li [5] give experimental results for [0₂/90_n]_s crossply layups. The material data were as given in the previous example. An estimation for the delamination initiation strain has been calculated. The results are compared with the experimental results in the next table. Again we used G_{dc} of 130 N/m. The ply thickness was reported to be 0.132 mm.

Layup	E_1 [GPa]	E_d [GPa]	ϵ_c [-]	ϵ_c [mm/m] experim.
[0/0/90]+[90/0/0]	101	100.7	.030	>.0123
[0/0/90 ₃]+[90/0/0] ¹⁾	78.7	78.5	.035	>.0100
[0/0/90 ₇]+[90/0/0] ¹⁾	56.4	56.3	.030	.0080
[0/0]+[0/0/90 ₁₆]+[0/0] ²⁾	38.5	38.5	.038	.0041

¹⁾ two alternating delaminations ²⁾ two continuous delaminations

From the calculations follows that delamination is most likely on the plane of symmetry for $[0_2/90]_s$ and near the 0/90 interface for the thicker specimens. For the thickest laminate two continuous delaminations at the 0/90 interface are predicted. The order of the predicted initiation strain is much higher than the strains where matrix cracking, 0-ply splitting and fibre break occur. The calculated values are nearly the same for all thicknesses. It is likely that in this case there is a strong interaction with the other damage modes.

4 DISCUSSION AND RECOMMENDATIONS

In the previous chapter we have applied the reduced stiffness method on layups of three different graphite epoxies. The results are very good and the advantage is that it is not necessary to calculate detailed stresses in the other directions and to calculate local stresses at the side surfaces of the plate.

We found that the discrepancy between Finite Element calculations and the reduced stiffness method observed by Schellekens was caused by the fact that he used different boundary conditions in both approaches. If the correct (natural, see Appendix 1) boundary conditions are used the results match very good.

From the calculations also follows that with the same energy release rate G_{dc} the results for different lay-ups can be predicted. Only for situations where the delamination initiation strain is higher than the strain where other damages like matrix cracking and fibre cracking initiate, the results are poor because there is an interaction with these other damages.

The reduced stiffness method can very well be used in design. It is not yet clear whether it is possible to apply the method in a rigorous way in the Finite Element Method in situations with varying stresses.

It is possible, that the onset of delamination will be different for the stresses in the two perpendicular directions of the laminate. In cases with one large stress component there is probably no problem, but in cases where both stresses are near to the delamination initiation stress, the two will interact. This problem of interaction has to be solved before an implementation in a Finite Element Method can be used in a rigorous way.

5 LITERATURE

- [1] O'Brien, T.K.; Characterization of Delamination; Onset and Growth in a Composite Laminate; *Damage in Composite Materials*; ASTM STP 775; K.L. Reifsneider, ed.; pp. 140-167 (1982).
- [2] Eikhoff J. v. d.; Paas M.H.J.W.; Numerical Solution of failure processes in Composite Laminates by Continuum Damage Mechanics; TNO-report B92-0433.
- [3] Schellekens, L.C.J., Borst R. de; Application of linear and nonlinear fracture mechanics options to free edge delamination in laminated composites; *Computational mechanics: Recent developments in DIANA*; HERON Volume 36 1991 no 2.
- [4] Crossman, F.W.; Wang A.S.D.; The Dependence of Transverse Cracking and Delamination on ply Thickness in Graphite/Epoxy Laminates; *Damage in Composite Materials*; ASTM STP 775; K.L. Reifsneider, ed.; pp. 118-139 (1982).
- [5] Wang, A.S.D., Kishore N.N., Li, C.A. (1985) Crack Development in Graphite-Epoxy Cross-ply Laminates under Uniaxial Tension, *Comp. Science Techn.*, **24**, 1-31.

Appendix 1 Longitudinal laminate stiffness for "Natural boundary conditions"

For the "natural boundary conditions" discussed in Chapter 2 we can derive the longitudinal laminate stiffness. First rearrange the relation between forces/moments and strains/curvatures such that we have second the terms with zero forces/moments and last the term with zero strains/curvatures:

$$\begin{bmatrix} N_x \\ 0 \\ 0 \\ N_{xy} \\ M_x \\ M_{xy} \end{bmatrix} = \begin{bmatrix} S_{11} & S_{12}^T & S_{13}^T \\ S_{12} & S_{22} & S_{23}^T \\ S_{13} & S_{23} & S_{33} \end{bmatrix} \begin{bmatrix} \epsilon_x \\ \epsilon_y \\ \kappa_y \\ 0 \\ 0 \\ 0 \end{bmatrix}$$

Because we are only interested in N_x and ϵ_x we eliminate ϵ_y and κ_y , giving:

$$\sigma_x = \frac{N_x}{T} = [S_{11} - S_{12}^T S_{22}^{-1} S_{12}] \frac{\epsilon_x}{T}$$

where:

T: Total laminate thickness.

This equation gives the required longitudinal laminate stiffness term.

Appendix 2 Longitudinal laminate stiffness for "Alternating delamination boundary conditions"

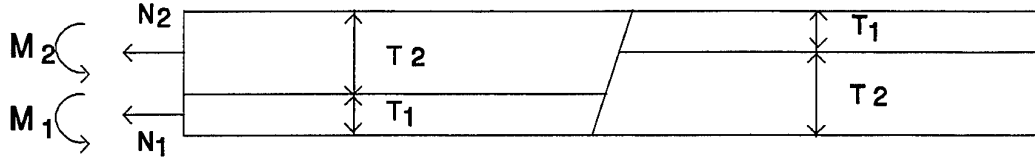
For the "alternating delamination boundary conditions" discussed in Chapter 2 we can derive the longitudinal laminate stiffness. Again rearrange the relation between forces/moments and strains/curvatures such that we have second the terms with zero forces/moments and last the term with zero strains/curvatures:

$$\begin{bmatrix} N_x \\ M_x \\ 0 \\ 0 \\ N_{xy} \\ M_{xy} \end{bmatrix} = \begin{bmatrix} S_{11} & S_{12}^T & S_{13}^T \\ S_{12} & S_{22} & S_{23}^T \\ S_{13} & S_{23} & S_{33} \end{bmatrix} \begin{bmatrix} \epsilon_x \\ \kappa_x \\ \epsilon_y \\ \kappa_y \\ 0 \\ 0 \end{bmatrix}$$

Again we eliminate ϵ_y and κ_y , giving:

$$\begin{bmatrix} N_x \\ M_x \end{bmatrix} = \begin{bmatrix} S_{11} & -S_{12}^T S_{22}^{-1} S_{12} \end{bmatrix} \begin{bmatrix} \epsilon_x \\ \kappa_x \end{bmatrix} = \begin{bmatrix} E_{ff} & E_{gf} \\ E_{gf}^T & E_{gg} \end{bmatrix} \begin{bmatrix} \epsilon_x \\ \kappa_x \end{bmatrix}$$

In the delaminated laminate we now have the situation as indicated in the following figure of a deformed laminate:



We have two parts of the delaminated laminate on top of each other. We assume that the surface between the two opposite delaminated areas remains straight. In that case we get the following relation between the local midplane strains and the global midplane strain and curvature:

$$\begin{aligned} \epsilon_1 &= \epsilon - \kappa \frac{T_2}{2} \\ \epsilon_2 &= \epsilon + \kappa \frac{T_1}{2} \end{aligned}$$

where:

- ϵ : strain at the midplane of the total laminate;
- κ : curvature in the delaminated parts;
- ϵ_i : strain in the midplane of part i;
- T_i : Thickness of part i.

Now the forces and moments on the two parts can be calculated:

$$\begin{aligned} N_1 &= E_{ff1} \epsilon + (E_{gf1} - \frac{T_2}{2} E_1) \\ N_2 &= E_{ff2} \epsilon + (E_{gf2} + \frac{T_1}{2} E_2) \\ M_1 &= E_{gf1} \epsilon + (E_{gg1} - \frac{T_2}{2} E_{gf1}) \\ M_2 &= E_{gf2} \epsilon + (E_{gg2} + \frac{T_1}{2} E_{gf2}) \end{aligned}$$

It is now possible to have no external moment and a mean curvature over adjacent parts of zero. This means that:

$$M_1 + M_2 = N_1 \frac{T_2}{2} - N_2 \frac{T_1}{2}$$

We now eliminate the curvature:

$$\begin{aligned} \kappa &= - \frac{f_2}{f_{42} + 2 f_{41} + f_{61}} \varepsilon \\ f_2 &= E_{gf1} + E_{gf2} - \frac{T_2}{2} E_{ff1} + \frac{T_1}{2} E_{ff2} \\ f_{41} &= - \frac{T_2}{2} E_{gf1} + \frac{T_1}{2} E_{gf2} \\ f_{42} &= E_{gg1} + E_{gg2} \\ f_{61} &= \frac{T_2^2}{4} E_{ff1} + \frac{T_1^2}{4} E_{ff2} \end{aligned}$$

The global stress can now be calculated:

$$\begin{aligned} \sigma &= \frac{N_1 + N_2}{T_1 + T_2} = \frac{\varepsilon}{T_1 + T_2} \left(f_1 - \frac{f_2^2}{f_{42} + 2 f_{41} + f_{61}} \right) \\ f_1 &= E_{ff1} + E_{ff2} \end{aligned}$$

from which the longitudinal laminate stiffness follows.

Appendix 3 Longitudinal laminate stiffness for "moment free boundary conditions"

For the "moment free boundary conditions discussed in Chapter 2 we can derive the longitudinal laminate stiffness. This is done by eliminating the curvatures from (9) giving:

$$N = [A - B^T D^{-1} B] \varepsilon$$

from which the strain can be calculated with matrix inversion:

$$\varepsilon = [A - B^T D^{-1} B]^{-1} N = A' N$$

With $N_{xy}=0$ the longitudinal laminate stiffness follows:

$$\sigma = \frac{1}{A'_{11} T}$$

Appendix 4 Longitudinal laminate stiffness for "curvature free boundary conditions"

For the "curvature free boundary conditions discussed in Chapter 2 we can derive the longitudinal laminate stiffness. This is done by matrix inversion using (9) giving:

$$\varepsilon = A^{-1} N$$

The longitudinal laminate stiffness follows with $N_y=0$:

$$\sigma = \frac{1}{A^{-1}_{11}} T$$

REPORT DOCUMENTATION PAGE		
1. DEFENCE REPORT NUMBER (MOD-NL) RP 96 - 108	2. RECIPIENT'S ACCESSION NUMBER	3. PERFORMING ORGANIZATION REPORT NUMBER 93-CMC-R0786
4. PROJECT/TASK/WORK UNIT NO. 42775554	5. CONTRACT NUMBER A92/KM/178	6. REPORT DATE 30 August 1996
7. NUMBER OF PAGES 22	8. NUMBER OF REFERENCES 5	9. TYPE OF REPORT AND DATES COVERED Final Report
10. TITLE AND SUBTITLE Reduced stiffness method for onset of delamination		
11. AUTHOR(S) J. v.d. Eikhoff		
12. PERFORMING ORGANIZATION NAME(S) AND ADDRESS(ES) Centre for Mechanical Engineering Leeghwaterstraat 5 2628 CA DELFT, The Netherlands		
13. SPONSORING/MONITORING AGENCY NAME(S) AND ADDRESSES(S) Sponsor: Netherlands Ministry of Defence Monitoring agency: TNO Defence Research, Schoemakerstraat 97, 2628 VK DELFT, The Netherlands		
14. SUPPLEMENTARY NOTES The Centre for Mechanical Engineering is part of TNO Building and Construction Research The classification designation ongerubriceerd is equivalent to Unclassified.		
15. ABSTRACT (MAXIMUM 200 WORDS, 1044 BYTES) The reduced stiffness method has been used to determine the onset of delamination for a number of different layups of AS4/3501.6, T300/934 and T300/5208 graphite epoxy plates. The results are very good. The advantage is that it is not necessary to calculate detailed stresses in the third direction and to calculate local stresses at the surface of the plate. In order to make the method applicable for the Finite Element Method it is necessary to investigate situations with varying stresses. Also it is likely, that the onset of delamination will be different for the stresses in the two perpendicular directions of the laminate. In cases where both stresses are near to the delamination initiation stress, the two probably will interact. Also the interaction between transverse matrix cracking and delamination has to be investigated further.		
16. DESCRIPTORS Mechanical properties Computer program		IDENTIFIERS Strength; GRP Continuum Damage Mechanics
17a. SECURITY CLASSIFICATION (OF REPORT) ongerubriceerd	17b. SECURITY CLASSIFICATION (OF PAGE) ongerubriceerd	17c. SECURITY CLASSIFICATION (OF ABSTRACT) ongerubriceerd
18. DISTRIBUTION/AVAILABILITY STATEMENT Unlimited availability, requests shall be referred to sponsor		17d. SECURITY CLASSIFICATION (OF TITLES) ongerubriceerd

Distributielijst bij rapport 93-CMC-R0786
Instituut: TNO Bouw, CMC
Project A92/KM/178

DWOO	1
HWO-Centrale Organisatie	(B)
HWO-KM	1
HWO-KL	(B)
HWO-KLu	(B)
Projectbegeleider DMKM, afd. Scheepsbouw, ir. T.N. Bosman	4
Bureau TNO-DO	1
Bibliotheek KMA	3
Centrum voor Mechanische Constructies	8

(B) = Beperkt rapport